Vol. 196: 127–141, 2000 | MARINE ECOLOGY PROGRESS SERIES
Mar Ecol Prog Ser | Published April 18

Simulation of the effects of naturally enhanced UV radiation on photosynthesis of Antarctic phytoplankton

Astrid U. Bracher*, Christian Wiencke

Alfred-Wegener-Institute for Polar and Marine Research, Postfach 120161, 27515 Bremerhaven, Germany

ABSTRACT: The effects of spectral exposure corresponding to normal and depleted stratospheric ozone concentrations on photosynthesis and mycosporine-like amino acids (MAAs) contents of different natural phytoplankton communities were studied in early austral summer 1995/1996 during the JGOFS ANT XIII/2 cruise in the Atlantic Sector of the Southern Ocean. The radiation conditions were simulated in a special solar simulator in which the same sample was incubated under 2 light regimes differing in UV-B doses. In all phytoplankton samples the quantum yield of electron transport in photosystem II (PSII) decreased after incubation under increased ultraviolet radiation (UVR) levels. Only samples outside of phytoplankton blooms showed a significant lowering of photosynthetic production rate due to enhanced UV-B. Phytoplankton cells within the blooms probably received protection from UV-absorbing MAAs, because only there cells, chains or colonies of phytoplankton communities were large enough to act in combination with MAAs as effective sunscreens. In addition, within the blooms, due to shallow upper mixed layers (UMLS) and stability within the water column, cells had probably enough light to maintain turnover rates of repair mechanisms at PSII and induce sufficient MAA synthesis; these processes were able to compensate for the negative effects of UVR. In contrast, the damaging effect on photosynthesis was much more severe on phytoplankton cells outside the blooms; most cells (70 to 90%) here were too small to receive protection from the MAAs present, and UMLs were deep and mixing rates high.

KEY WORDS: UV radiation · Antarctica · Phytoplankton · Photosynthesis · Photoinhibition · Photodamage · Mycosporine-like amino acids

INTRODUCTION

Serious concerns exist regarding depletion of atmospheric ozone (O_3) associated enhancement of ultraviolet-B radiation (UV-B), and its impact on marine primary productivity (Smith et al. 1992). High-latitude oceans are considered most at risk from negative effects of increasing UV-B because the polar latitudes are experiencing the greatest changes in UV-B, and the endemic flora has evolved under conditions relatively low in UV-B (Frederick & Snell 1988, Vincent & Roy 1993). UV-B is known to have various deleterious effects on plants, including the microscopic algae that account for the bulk of the oceans primary production (Holm-Hansen et al. 1993, Vincent & Roy 1993): UV-B damages the reaction centre of photosystem II (PSII) and the carboxylating enzyme, ribulose biphosphate carboxylase/oxygenase (RUBISCO; Iwanzik et al. 1983, Greenberg et al. 1989, Strid et al. 1990, Tevini 1994, Wilson et al. 1995, Hanelt 1996). Other sites in the photosynthetic apparatus may also be at risk (Nogues & Baker 1995), and diminished chlorophyll *a* concentration (chl *a*) has been documented (Strid et al. 1990). Short-term exposure (< natural photoperiod) commonly reduces photosynthetic rates in algae studied to date from temperate zones (Cullen & Lesser 1991, Ekelund 1994, Lesser et al. 1994), and recent reports indicate similar effects on Antarctic marine microalgae (Neale et al. 1994, Schofield et al. 1995).

*E-mail: abracher@awi-bremerhaven.de

In addition to the fact that photosynthetic carbon incorporation in waters around Antarctica and in temperate latitudes is significantly diminished by UV-B even at present levels (Helbling et al. 1992, Ryan 1992, Smith et al. 1992, Holm-Hansen et al. 1993, Neale et al. 1994), it has also been found that phytoplankton production is sensitive to spectral shifts in UV radiation (UVR) (Neale et al. 1992, Boucher & Prezelin 1996). The irradiance field within the water column of the Southern Ocean is not only very heterogeneous with respect to intensity due to season, time of the day, cloud and ice cover, but also with respect to quality due to change of spatial distribution of the ozone hole (Roy et al. 1994) and the absorbing components in the water (Bracher & Tilzer 2000).

Until now studies looking at the effect of increased UV-B levels on phytoplankton photosynthesis from the Southern Ocean were performed using the following methods: phytoplankton were incubated either *in situ* or in outdoor enclosures under the full solar spectrum including UV and compared to solar spectra excluding different wavelengths of UVR (El-Sayed et al. 1990, Helbling et al. 1992, Neale et al. 1992, Smith et al. 1992, Holm-Hansen et al. 1993, Boucher & Prezelin 1996, Helbling et al. 1996) or under artificial light (Cullen & Lesser 1991, Davidson & Marchant 1994, Davidson et al. 1996). In the latter case the intensity in the UVR range was far too high or unnatural wavelengths (e.g., <290 nm) were present in the spectra. In both methods, with respect to spectral quality and quantity, phytoplankton were not exposed to the irradiance field encountered in the water column corresponding to variations in the solar spectrum due to various stratospheric ozone concentrations. Only Prezelin et al. (1994) compared effects of primary production for normal and depleted ozone concentrations, but different samples were compared with each other. Therefore, the objective of this study was to study production rates and quantum yield of electron transport in PSII under the influence of an irradiance field almost corresponding to the natural irradiance conditions under normal and depleted ozone concentrations on the same natural phytoplankton samples. In order to simulate the radiation conditions under stratospheric ozone depletion, a newly constructed solar simulator was used. The differences in response of the samples to UVR were evaluated by considering several biotic (photosynthetic compounds, species composition, size fraction) and abiotic (hydrography) conditions. In addition to that, UV-B absorbing compounds present prior to the experiment in these samples were identified and their potential to act in the various samples as effective UV-sunscreens was discussed. The results of this study will contribute to the understanding of how increased UV-B radiation due to stratospheric ozone depletion affects carbon fluxes in the Southern Ocean.

MATERIALS AND METHODS

Our data were collected during the Southern Ocean JGOFS cruise ANT XIII/2 (December 1995 to January 1996) in the area 49°–67° S, and 6° W–12° E in the Atlantic sector of the Southern Ocean with the RV 'Polarstern' (Fig. 1). Samples were taken at 23 stations during the cruise. All stations were in the open ocean without any ice cover. *In situ* water samples were restricted to the upper 120 m of the water column.

Light measurements and ozone concentration during the cruise. Vertical profiles of the downwelling spectral distribution of the underwater light field were measured to 120 m depth as described in detail in Bracher & Tilzer (2000) using a MER-2040 underwater spectroradiometer equipped with a cosine collector (Biospherical Instruments, San Diego, USA). Spectral light intensities were measured at wavelengths of 340, 380, 412, 443, 465, 490, 510, 520, 550, 560, 615, 633, 665 and 683 nm (10 nm bandwidth) at all sampled CTD stations and as a reference on deck with a second spectroradiometer MER-2041.

Photosynthetically active radiation (PAR) (400–700 nm) and UV-A (320–400 nm) and UV-B (280–320 nm) radiation were continuously measured on deck throughout

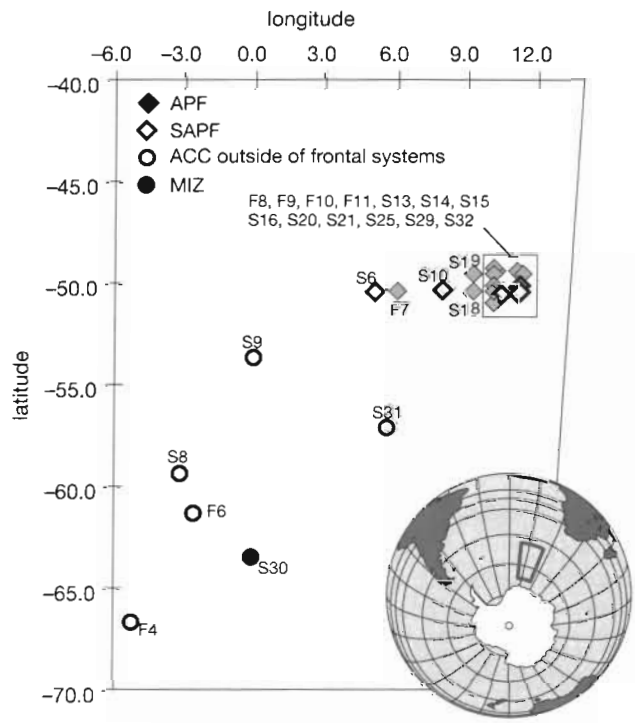

Fig. 1. Area in which Southern Ocean JGOFS cruise ANT XIII/2 (December 1995 to January 1996) data were collected for this study. Stations were located in the Antarctic Polar Front (APF), south of the APF (SAPF), Antarctic Circumpolar Current outside of frontal systems (ACC) and the Marginal Ice Zone (MIZ) within the Atlantic sector of the Southern Ocean

the cruise. PAR was measured with a Li-Cor sensor (Li-193SA) and the UV light with a bandpass radiometer (RM-21, Gröbel, Karlsruhe, Germany) equipped with broadband UV-A and UV-B cosine sensors. The sensors were mounted on the top of the ship in a place where they were not shaded by the ship's superstructure. Every 10 min PAR (in µmol photons m^{-2} s^{-1}) means and UV-A and UV-B radiation means (in W m^{-2}) were logged throughout the day to a Li-Cor LI-1000 Data Logger and a 486 Compaq computer, respectively. PAR values measured in air (E_a[PAR]) were converted into values at the subsurface (E_0[PAR]) by using the equation $E_0[PAR] = E_a[PAR] \cdot c$. The conversion factor c was determined by comparison of the MER underwater PAR irradiance measurements with the on-line Li-Cor measurements and was equal to 0.75621 ± 0.05149 (n = 20). E_0[PAR] at the CTD stations were determined by integrating irradiance fluxes in the 12 wavelengths measured and assuming that they were valid for the entire waveband in whose mid-point irradiance was measured. PAR values at 5 m, E_5[PAR], at the sampled station during the day of sampling were determined as follows:

$$E_5[PAR](t) = E_0[PAR] \cdot \exp(-k_5[PAR] \cdot 5) \quad (1)$$

The specific vertical attenuation coefficients of PAR at 5 m depth, k_5[PAR], were determined from the expression in Smith & Baker (1978) for deriving k_d at a specific wavelength:

$$-k_5[PAR] = (\ln E_5[PAR] - \ln E_0[PAR])/5 \quad (2)$$

Because we were not able to measure UV-B in the water column at that time, we used the extraterrestrial solar radiation field as input for an atmospheric model together with attenuation coefficients for clear seawater to compute an approximate value for the *in situ* light field at 5 m depth, $E_5^{calc}[\lambda]$. The calculation is based on the solar spectrum, J_0, given by Labs & Neckel (1984) applied to the atmospheric model for clear sky conditions used by Tüg (1978) and modified by Rieper (1996) regarding the actual airmass, m, with $m = 1/\cos z$, where z is the solar zenith angle. The ozone concentration at each time and location were taken from currently available data of the Tiros Operational Vertical Sounder (TOVS) aboard the NOAA satellite. Light loss in the water column was calculated from the spectral attenuation coefficients $k_w[\lambda]$ given by Smith & Baker (1981), not regarding scattering and reflection. Light loss in the atmosphere is characterised by the 3 extinction coefficients of Rayleigh scattering, $k_{RAY}[\lambda]$, aerosol absorption (and scattering), $k_{AER}[\lambda]$, and ozone absorption, $k_{OZON}[\lambda]$ (see Eq. 3). Atmospheric absorption bands from oxygen and water vapour were neglected.

$$E_5^{calc}[\lambda] = J_0 \cdot \exp\left(-\left\{\left[k_{AER}[\lambda] + k_{RAY}[\lambda] + (k_{OZON}[\lambda] \cdot du/1000)\right] \cdot m\right\}\right) \cdot \exp\left[-(k_w[\lambda] \cdot 5)\right] \quad (3)$$

with $k_{AER}[\lambda] = A_0 \cdot \lambda^{-\alpha} \cdot 0.9212$ (A_0 = characteristic aerosol portion [0.25] and α = 0.81); $k_{RAY}[\lambda] = 0.0094977 \cdot (1/\lambda)^4 \cdot \{0.23465 + 107.6/[146 - (1/\lambda)^2] + 0.93161/[41 - (1/\lambda)^2]\} \cdot 0.9212$; $k_{OZON}[\lambda]$ is given by Labs et al. (1987); and du = thickness of ozone layer in Dobson Units.

The calculated light fields are approximating maximum light conditions at the sampled stations. Therefore, in order to prove if these data were corresponding to the *in situ* irradiance conditions at the sampled stations, the maximum values of E_5[PAR] at the sampled station and during the day of sampling, measured with the MER 2040 instrument and converted as described above, was compared to the approximate *in situ* underwater irradiance of PAR. There was a good correspondence between the two during clear sky conditions at the sampled station (Fig. 2, r = 0.92). Therefore the approximate *in situ* underwater irradiance at 5 m depths was comparable to the irradiance values used during incubations.

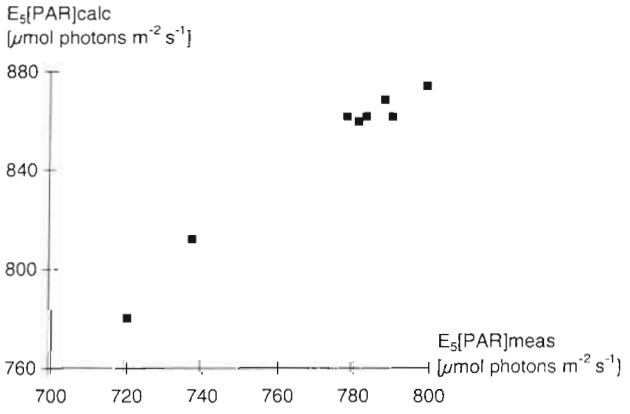

Fig. 2. Comparison of the maximum *in situ* underwater irradiance of PAR at 5 m depth measured at the sampled stations at the day of sampling (E_5[PAR]meas) and the approximate *in situ* underwater irradiance (E_5[PAR]calc). Values of E_5[PAR]calc were been calculated by the spectral-resolving-irradiance model of Tüg (1978) modified by Rieper (1996) under clear sky conditions based on the specific stratospheric ozone concentration. Only values of sampled stations where clear sky conditions occurred were used for comparison

Water sample analysis and experiments. The following measurements were carried out using water sampled from a Bio-Rosette at CTD stations and surface water samples taken with a bucket at other stations. At CTD stations (S6, S8, S9, S10, S13, S14, S16, S18, S19, S20, S21, S25, S29, S30, S31, S32; Fig. 1, Table 1) the measurements of chl *a*, mycosporine-like amino acids (MAAs) and quantum yield of electron transport in photosystem II (PSII) were carried out using water samples from 6 depths within the euphotic zone. At all other stations (F4, F6–F11) only 1 sample for each measurement was taken from the surface water.

Table 1. List of sampled stations during ANT XIII/2 including position, date and time and ozone concentration (O_3) in Dobson units (DU). S: stations where samples were taken from the vertical profile; F: stations where only surface samples were taken

Stn	Longitude	Latitude	Sampling date (d.mo.yr) and time	O_3 (DU)
S6	05.31	−50.22	9.12.95 12:30 h	240–270
S8	−03.13	−59.26	12.12.95 11:00 h	270–300
S9	−00.06	−53.60	22.12.95 17:40 h	270–300
S10	08.09	−50.29	25.12.95 21:45 h	270–300
S13	11.32	−49.54	29.12.95 14:00 h	270–300
S14	11.32	−50.18	30.12.95 03:00 h	270–300
S16	10.17	−51.06	30.12.95 18:00 h	300–330
S18	09.34	−50.42	5.1.95 08:00 h	300–330
S19	09.34	−49.54	5.1.95 23:45 h	300–330
S20	10.18	−49.30	6.1.95 06:30 h	300–330
S21	10.18	−49.54	6.1.95 15:30 h	300–330
S25	10.18	−50.18	7.1.95 05:30 h	270–300
S29	10.18	−50.42	7.1.95 23:00 h	270–300
S30	00.00	−63.40	16.1.95 10:00 h	300–330
S31	05.50	−57.20	17.1.95 16:30 h	300–330
S32	11.33	−49.54	20.1.95 06:00 h	270–300
F4	−05.08	−66.55	20.12.95 05:00 h	300–330
F6	−02.40	−61.46	21.12.95 05:00 h	300–330
F7	06.00	−50.42	24.12.95 07:00 h	270–300
F8	10.24	−49.38	27.12.95 19:00 h	270–300
F9	11.20	−49.41	1.1.95 09:00 h	270–300
F10	10.50	−50.47	2.1.95 11:00 h	270–300
F11	10.17	−49.50	3.1.95 13:00 h	300–330

Chlorophyll data from the cruise were obtained from Lucas et al. (1997) and Hense et al. (1998). Chlorophyll and phaeophytin concentrations were analysed using the method of Evans et al. (1987). Determinations were performed by filtering water samples onto 25 mm Whatman GF/F filters, extracting pigments retained on the filters in 9 ml 90:10 acetone:water for 2 to 3 h in a dark refrigerator and reading fluorescence, after grinding, on a Turner Designs scaling fluorometer before and after acidification with 2 drops of 5% 1 N HCl.

Quantum yield of electron transport in PSII. Quantum yield of electron transport in PSII was determined by measuring variable fluorescence of PSII with a PAM-100 device (WALZ, Effeltrich, Germany). Maximum quantum yield of electron transport in PSII (i.e., excitation capture by open PSII centres) was calculated as the ratio of variable to maximum fluorescence (F_v/F_m) of the dark acclimated algae. The information given by the F_v/F_m value is a measure of quantum yield of electron transport in PSII and can be used as an index of the photosynthetic conversion efficiencies of phytoplankton (Schreiber et al. 1995). About 1 ml of sample was incubated in a ice-cold water cuvette. After application of a 5 s far-red pulse (30 µmol photons m^{-2} s^{-1}) to reoxodise the electron transport chain, the samples were kept in darkness for 5 min to extinguish energy-dependent fluorescence quenching (qE) and quenching by state transitions (qT). Then minimal fluorescence (F_0) was measured with a pulse measuring beam (approximately 0.3 µmol photons m^{-2} s^{-1}, 650 nm). Afterwards a short pulse of saturating white light (0.4 to 0.8 s, 1500 µmol photons m^{-2} s^{-1}) was provided to determine F_m. Each measurement was repeated 3 times.

Influence of enhanced UV-radiation on phytoplankton photosynthesis. Water samples from the surface were taken for determination of the effect of UV radiation on photosynthesis. In addition, at CTD stations photosynthetic rates were also determined in water samples from the 1% light depth. To measure the photosynthetic rate, 50 ml of sample were spiked with 10 µCi of ^{14}C (triplex and dark sample). These samples and an unspiked sample for measuring F_v/F_m, as described above were illuminated in quartz bottles in a laboratory incubator, called a solar simulator, to a radiation field simulating stratospheric ozone depletion (corresponding to 180 DU) in 5 m water depth at the sampled location. The samples were incubated over 4 h at *in situ* temperature with a constant photon fluence rate of PAR between 350 and 500 µmol photons m^{-2} s^{-1}. All samples were exposed to irradiance conditions corresponding to a saturated light field (irradiance $E > E_k$), the light saturation parameter E_k was determined by photosynthesis-versus-irradiance curves in a PAR incubator during the cruise (Bracher et al. 1999). The solar simulator has been previously described by Tüg (1996) and Abele-Oeschger et al. (1997) and the solar simulator's irradiance field is based on a spectrum calculated in accordance to the spectral-resolving-irradiance model of Tüg (1978) modified by Rieper (1996). Both samples (from the subsurface and the 1% light depth) were incubated under the same irradiance field in order to study differences in sensitivity to enhanced levels of UVR. We used the irradiance field corresponding to 5 m depth because of technical constraints. The samples were illuminated with a 400 W Metallogen lamp (Phillips MSR 400 HR) containing a number of lanthanide rare earths, resulting in a solar-like continuum. The parallel light beam passed from above through a wire screen, which diminished the light intensity without changing the spectrum, 3 liquid filters with quartz windows, and a diffuser plate. The different liquids in these filters were aqueous solutions of K_2CrO_4, $CuSO_4$ and KNO_3. As the liquid filters were variable in thickness, using the different extinction coefficients almost natural radiation conditions could be simulated. The samples were positioned in a double-walled glass jar covered by a quartz plate and kept at *in situ* temperatures with a thermostat. UVR was measured under this plate by use of the RM-21 Groebel instrument and PAR using a Biospherical Instrument 4π probe (QSP200). The solar simulator was calibrated

prior to and after the cruise with an UV spectrometer and no significant difference was found between the 2 measurements (the lamp's lifetime predicted by the manufacturer is 700 h; we used the lamp for 185 h in total in our study). Prior to the incubation, F_v/F_m was measured for an aliquot which was acclimated for 30 min to darkness to derive a time-zero value ($t0$). The rest of the water sample was kept in the dark at *in situ* temperature until it was prepared as above, but incubated under radiation conditions present under normal stratospheric ozone concentration (corresponding to 360 DU). The concentrated sample for measuring F_v/F_m was kept in the dark for 4.5 h after incubation. After half an hour and then every hour F_v/F_m was measured and compared to the $t0$ value. ^{14}C spiked samples were filtered on Sartorius cellulose nitrate filters (0.45 µm pore size) and put under acid fume in a desiccator for 15 min to release unassimilated $^{14}CO_2$. Scintillation cocktail (Quickszint 361) was added to the filters prior to the radioactivity assay in a Packard 1900CA Tri-Carb Liquid Scintillation Counter. The uptake of ^{14}C labelled bicarbonate into acid-stable organic material was converted to biomass-specific rates using measured values of chl *a* and alkalinity (from Stoll et al. 1997) as in Strickland & Parsons (1972).

For all measurements of primary production rates and quantum yields of electron transport in PSII mean values and standard deviations were determined.

UV-absorbing compounds. UV-absorbing MAAs were determined by filtering 1 or 2 l samples through 25 mm Whatman GF/F filters. The filters were put in Eppendorf tubes and afterwards directly deep frozen in liquid nitrogen. They were then stored at −80°C for analysis 10 mo later. Filters were extracted for 4 h in 25% aqueous methanol (v/v) at 45°C. Following extraction, samples were centrifuged at 14 000 × *g* for 5 min.

Supernatants were used to measure total spectral absorption between 260 and 700 nm with an UV-visible spectrophotometer (Varian Cary 3) within an integrating sphere. The spectral range allowed estimates of UV-absorbing compounds. Photosynthetic pigments were not extracted in 25% aqueous methanol (v/v). Values of 'unpacked absorption' were derived according to Sosik & Mitchell (1991):

$$a(\lambda)\text{sol} = 2.3 \cdot \text{OD} \cdot \text{extracted volume}/(\text{pathlength of cuvette} \cdot \text{filtered volume}) \quad (4)$$

The value of maximum absorption in the UV range was determined (a_{UV}sol#) and corrected for the absorption due to water-soluble cell matter (e.g., cell debris, as are macromolecules of carbohydrates, proteins, amino acids, etc.) in the extract that is not due to MAAs, as suggested by Garcia-Pichel & Castenholz (1993):

$$a_{UV}\text{sol} = a_{UV}\text{sol\#} - a(260)\text{sol} \cdot (1.85 - 0.005\lambda) \quad (5)$$

where a_{UV}sol is the corrected value of maximum absorption in the UV range and $a(260)$sol is the absorption of the extract at 260 nm, and λ is the wavelength (in nm) of maximal absorbance.

After the measurements in the spectrophotometer were made, supernatants were evaporated to dryness under vacuum (Speed Vac Concentrator SVC 100H). The dried samples were re-dissolved in 200 µl of 100% methanol and vortexed for 30 s. Then, samples were analysed by high pressure liquid chromatography (HPLC) using a Waters 600 MS HPLC set-up, including gradient module with system controller and a Model 996 photodiodide array detector, according to the method of Nakamura et al. (1982) modified as follows: 20 µl of the sample were injected onto an HPLC column by an autosampler 717 plus. Separations of MAAs were performed on a stainless-steel Knauer Spherisorb SC8-column (5 µm; 4 mm inner diameter [i.d.]) protected with a SC-8 guard cartridge (20 mm × 4 mm i.d.). The mobile phase was 30% aqueous methanol (v/v) plus 0.1% acetic acid (v/v) and was run isocratically at a flow rate of 0.5 ml min^{-1}. MAAs were detected at 310 and 330 nm. Absorption spectra were recorded each second between 280 and 400 nm directly on the HPLC-separated peaks.

Identification was done using spectra and retention times compared to information from the literature (Dunlap & Chalker 1986, Caretto et al. 1990, Karentz et al. 1991, Shick et al. 1992) and with co-chromatography with standards extracted from marine red algae *Caloglossa stipitata* Post (shinorine and porphyra-334), *Chondrus crispus* (L.) Stackh. (shinorine/porphyra-334, palythine, palythinol, palythene), *Porphyra saldanhae* Stegenga Bolton Anderson (porphyra-334) and the cyanobacterial lichen *Peltula euploca* (Ach.) Poeltex Pišut (mycosporine-glycine), which were kindly provided by Dr. U. Karsten, AWI, Bremerhaven, Germany. Quantification of MAAs was done according to the formula from the Measurements Protocols of JGOFS (JGOFS 1993):

$$\text{conc. } (\mu g\ l^{-1}) = [A \cdot F \cdot 10^4/(E_n(1\%) \cdot I)] \quad (6)$$

with A = Area · min, F = flow velocity (ml min^{-1}), $E_n(1\%)$ = extinction coefficient (1%) from the literature (Table 2), and I = injection volume (ml).

RESULTS

Sampling sites

The geographical locations of the 3 different zones, the Antarctic Polar Front (APF), the Antarctic Circumpolar Current outside frontal systems and the Marginal Ice Zone (MIZ), within our cruise transect corre-

Table 2. Absorption maximum, molar extinction coeffient, *e*, and extinction coefficient (1%), E_n (1%), from the literature and our measurements for the mycosporine-like amino acids (MAAs) found in our study

MAA	Max. absorption Literature	Measured	*e*	E_n (1%)	Sources
Mycosporine-glycine	310	309.6	28 100	1145.9	Ito & Hirata (1977), Dunlap et al. (1986), Gleason (1993)
Porphyra-334	334	338.4	43 300	1250.2	Takano et al. (1979), Stochaj et al. (1994)
Shinorine	334	333.6	44 668	1344.1	Tsujino et al. (1980), Gleason (1993), Stochaj et al. (1994)
Palythine	320	319.2	36 200	1482.1	Takano et al. (1978a), Dunlap & Chalker (1986), Gleason (1993)
Palythinol	332	333.6	43 500	1438.8	Takano et al. (1978b), Dunlap & Chalker (1986)
Palythene	360	352.8	36 200	974.9	Takano et al. (1978b)

sponded to various biological features, based on data of size-fractionated chl *a* and pigment composition determined by HPLC analyses (Bracher et al. 1999) characterising the biomass and the structure of the phytoplankton community: The APF biomass was high (chl *a* went up to 1.83 mg m^{-3}), the >20 µm netplanktonic fraction made up >60% and diatoms dominated the total biomass with 60 to 80%. The highest biomass during this study was measured in the MIZ (up to 2.43 mg chl *a* m^{-3}) with prymnesiophytes, i.e., *Phaeocystis* sp. (M. Schültke pers. comm.), making up 50 to 60% and diatoms 30 to 40% of the phytoplankton biomass. Here, the >20 µm netplanktonic fraction (>60%) dominated the biomass. In contrast, in the Antarctic Circumpolar Current outside frontal systems maxima were below 0.80 mg chl *a* m^{-3} and the 2–20 µm fraction contributed 70% and the <2 µm fraction 20% to the biomass. Nine stations were within the Antarctic Circumpolar Current outside frontal systems; 4 stations (F10, S6, S10, S14) were located just south of the APF (SAPF, between 50.2° and 51.1° S), and 5 stations (F4, F6, S8, S9, S31) were located further south in this zone (>53.5°, referred to in the text as ACC). In the SAPF the diatom fraction of total biomass was only 25 to 45%, whereas dinoflagellate biomass made up 20 to 50%. Within the ACC, diatoms, dinoflagellates, prymnesiophytes and chrysophytes all contributed to the biomass. One station (S30) was in the open water of the MIZ and 13 stations (F7–F9, F11, S13, S16, S18–S21, S25, S29 and S32) were in the APF (Fig. 1, Table 1).

Stratospheric ozone concentrations and light conditions

Ozone concentrations during our cruise varied from 240 to 330 DU (Table 1). Daylengths ranged from 16 to 24 h and daily maxima of total PAR for the surface water from 440 to 2200 µmol photons m^{-2} s^{-1}. The maximum values of PAR were found in the ACC and MIZ; in the APF maximum values did not exceed 1500 µmol photons m^{-2} s^{-1}. The euphotic depth Z_{eu} ranged from 30 to 70 m. Stations within the ACC showed maximum values and stations of the APF gave minimum values for Z_{eu}. The station within the *Phaeocystis* sp. bloom (S30) also showed a low value for Z_{eu}, with 40 m (Bracher & Tilzer 2000). At 5 m the daily maximum UV-A ranged from 18.18 to 23.55 W m^{-2}, and the daily maximum UV-B from 0.33 to 0.62 W m^{-2}. Highest daily maxima for UV-A and UV-B were found in the APF, while lowest daily maxima for both were found at the southern most station in the ACC (F4) (Fig. 3a,b).

UVR values during experiments in the UV incubator are also shown in Fig. 3a,b. Values for incubations under high UVR (comparable to conditions under depleted stratospheric ozone concentrations) and under low UVR (comparable to conditions under normal stratospheric ozone concentrations) are just above/below the real values measured at 5 m depth. Fig. 4 shows an example of the lamp spectrum used in the incubator under depleted stratospheric ozone concentrations in the APF compared to a 'theoretical' sun spectrum under the same conditions (according to the spectral model of Tüg 1978 modified by Rieper 1996).

Quantum yield of electron transport in PSII and primary production rates

The quantum yield of electron transport in PSII, as indicated by F_v/F_m, reached in all samples very similar values under conditions simulating normal ozone as compared to the *t*0 values. For the spectral simulation under depleted ozone it decreased significantly (*t*-test, $p < 0.05$), between 23 and 88% compared to the *t*0 values (Fig. 5). F_v/F_m remained low even when kept in the dark for 4 h after exposure (data not shown).

The rates of photosynthesis of the incubations are shown in Fig. 6a,b. About half of the samples incubated under conditions simulating depleted ozone exhibited significantly lower production rates (30 to 65%) compared to the values derived under conditions simulating normal ozone concentrations. Samples within a bloom (such as samples from S18, S19, S21,

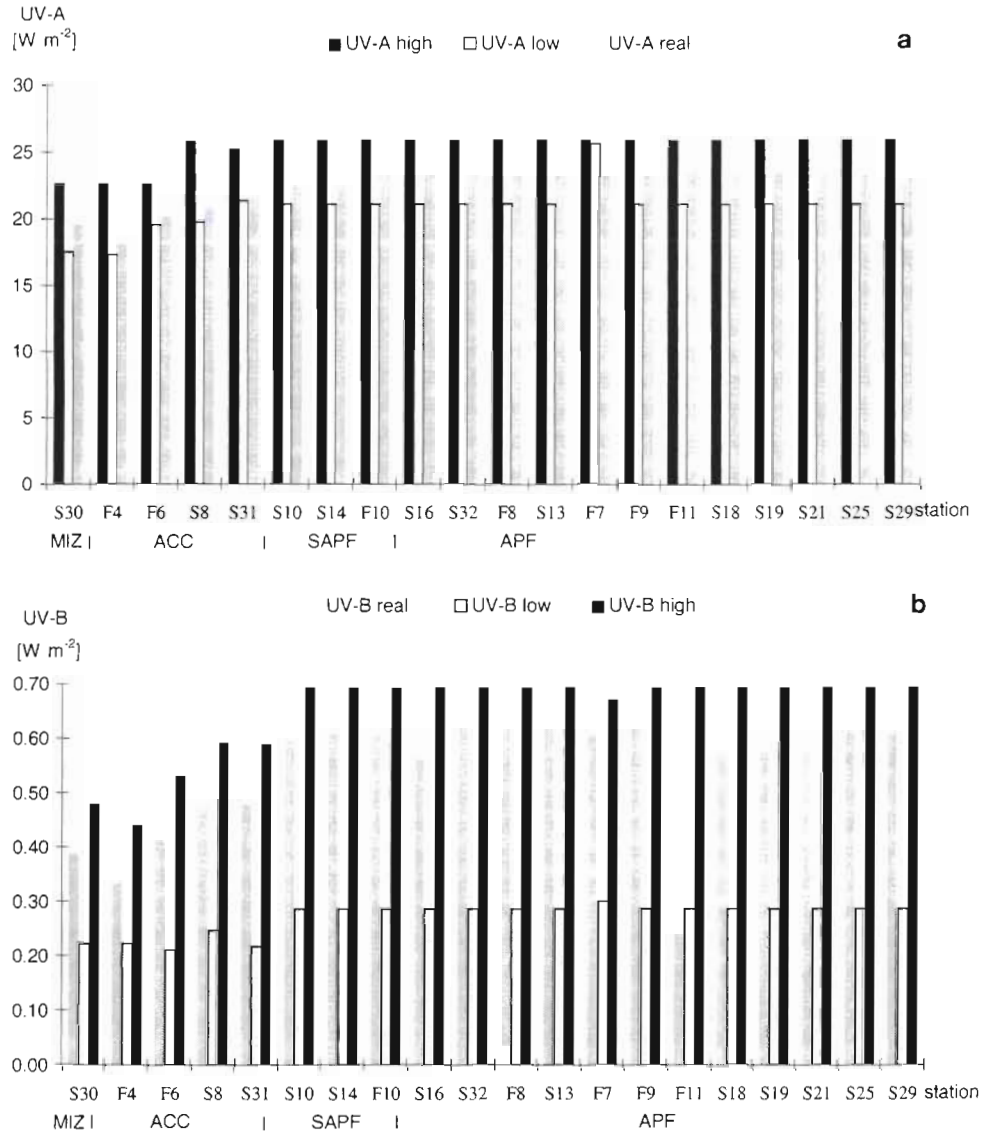

Fig. 3. (a) Ultraviolet-A radiation (UV-A) and (b) ultraviolet-B radiation (UV-B) calculated at 5 m depth by the spectral-resolving-irradiance model of Tüg (1978) modified by Rieper (1996) in accordance to measured ozone concentrations (TOVS-data) at the sampling sites (real UV-A/UV-B), and used in the incubations simulating the irradiance under depleted (high UV-A/UV-B) and normal ozone concentrations (low UV-A/UV-B). Stations are grouped into the areas within the Atlantic sector of the Southern Ocean in which they are located: MIZ, ACC, SAPF, APF

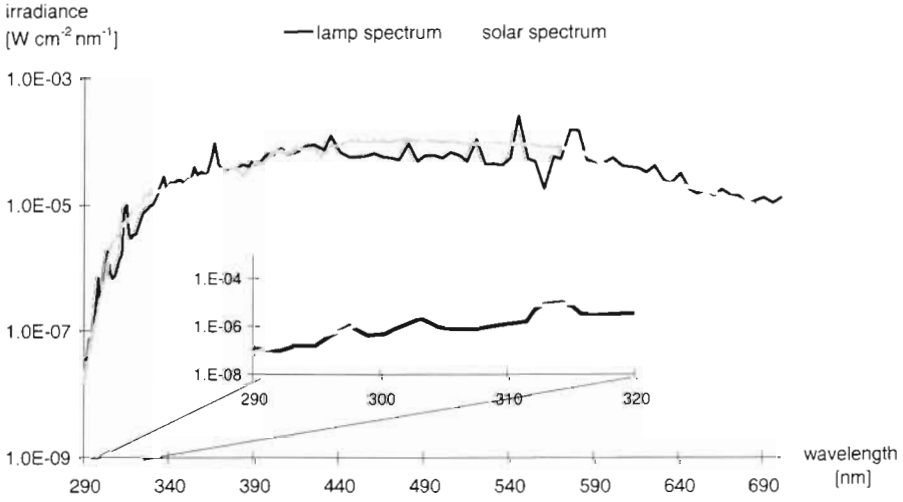

Fig. 4. Example of the lamp spectrum used for the incubation of water samples from Stn 21 (within the APF) simulating irradiance conditions at 5 m water depth under a depleted ozone concentration (180 DU) and actual sun spectrum under such conditions calculated using to the spectral model of Tüg (1978) modified by Rieper (1996) for the whole spectrum (290–700 nm) and for the UV-B region (290–320 nm)

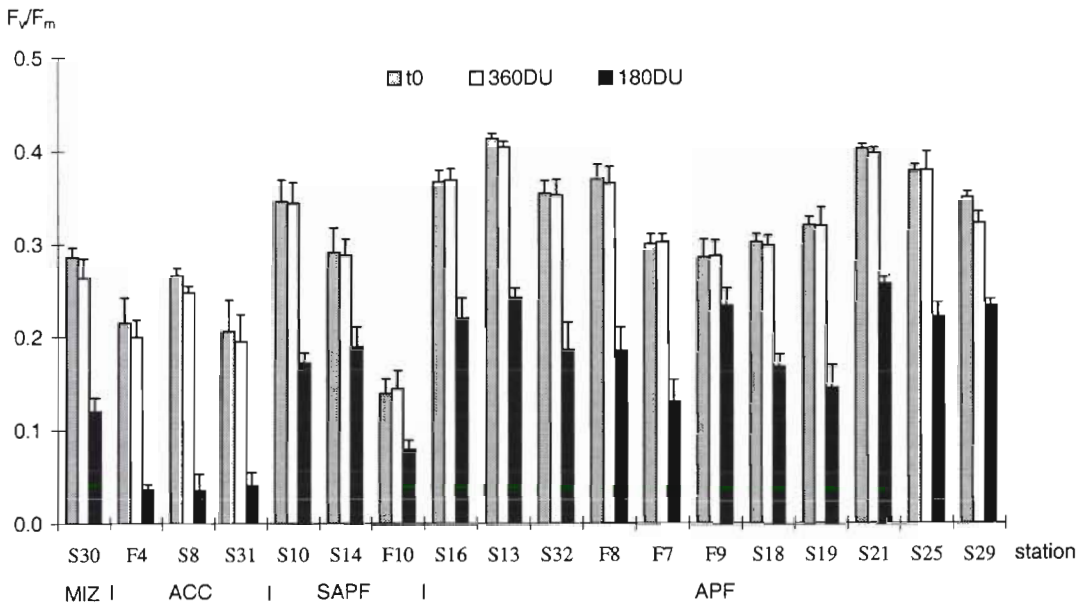

Fig. 5. Quantum yield of electron transport in PSII, F_v/F_m, in surface water samples after sampling ($t0$) and after 4 h of incubation under a spectrum corresponding to an irradiance field encountered at 5 m depth under depleted (180 DU) and normal ozone concentrations (360 DU). Stations are grouped to the areas within the Atlantic sector of the Southern Ocean in which they are located: MIZ, ACC, SAPF, APF

S25, S29, F7, F9 from the diatom bloom and S30 from the *Phaeocystis* sp. bloom) showed no significant difference in production rates (except for S21 at 29 m) between the 2 incubation conditions. The 3 stations close to SAPF, indicated by lower surface temperatures but still high chl *a* values (S16, F8 and at S32 only the surface), and the stations from the SAPF (S14, S10 and F10) showed significantly lower production rates under ozone hole conditions. Stations from further south in the ACC (F4, S8 and S31) showed the highest difference with a decrease above 50%. Significance level (*t*-test) was always $p < 0.05$, except for F10 and S10 (0 m), with $p < 0.1$.

Quality and quantity of MAAs

MAAs were found in nearly all samples, with the exception of samples from very high water depths with very low chl *a* content (Fig. 7a). We identified 6 types of MAAs: mycosporine-glycine, porphyra-334, shinorine, palythine, palythinol and palythene. Porphyra-334 made up 40 to 60% of the total concentration of MAAs. Palythine contributed around 20 to 30% and shinorine 10 to 20%. Very low values (<0.2 µg l^{-1}) of MAAs were found at the stations within the ACC (F4, F6, S8, S9, S31), while high values (>0.8 µg l^{-1}) were found within the *Phaeocystis* sp. bloom at the MIZ (S30) and within the diatom bloom at the APF (S13, S21, S25). Values of $a_{UV}sol$ (Fig. 7b) and $a(\lambda)sol$ (Fig. 7c) indicate the same trend, with high values at both phytoplankton blooms and low values outside the blooms, but variability among the stations within the APF differs in comparison to the MAA data.

DISCUSSION

Evaluation of experimental design

In this study UV effects on natural phytoplankton photosynthesis were tested by incubating the same sample under 2 simulated irradiance fields corresponding very closely to conditions under normal and depleted stratospheric ozone concentrations. A similar experiment was performed during ICECOLOR 1990 (Prezelin et al. 1994). However, in that study different samples were incubated under the 2 conditions and therefore the effects of the 2 irradiance conditions were not exactly comparable.

The irradiance spectra which were used for incubations simulating conditions of depleted ozone concentrations (180 DU) correspond well to conditions in our study area. TOVS data from the end of November 1995 showed in our part of the Atlantic sector ozone concentrations still below 200 DU (data not shown). Since the 'ozone hole' (defined as <200 DU) itself is continuously 'moving', at the same time, parts of Antarctica encounter high UV-B radiation due to low ozone concentrations (<200 DU), while others encounter low UV-

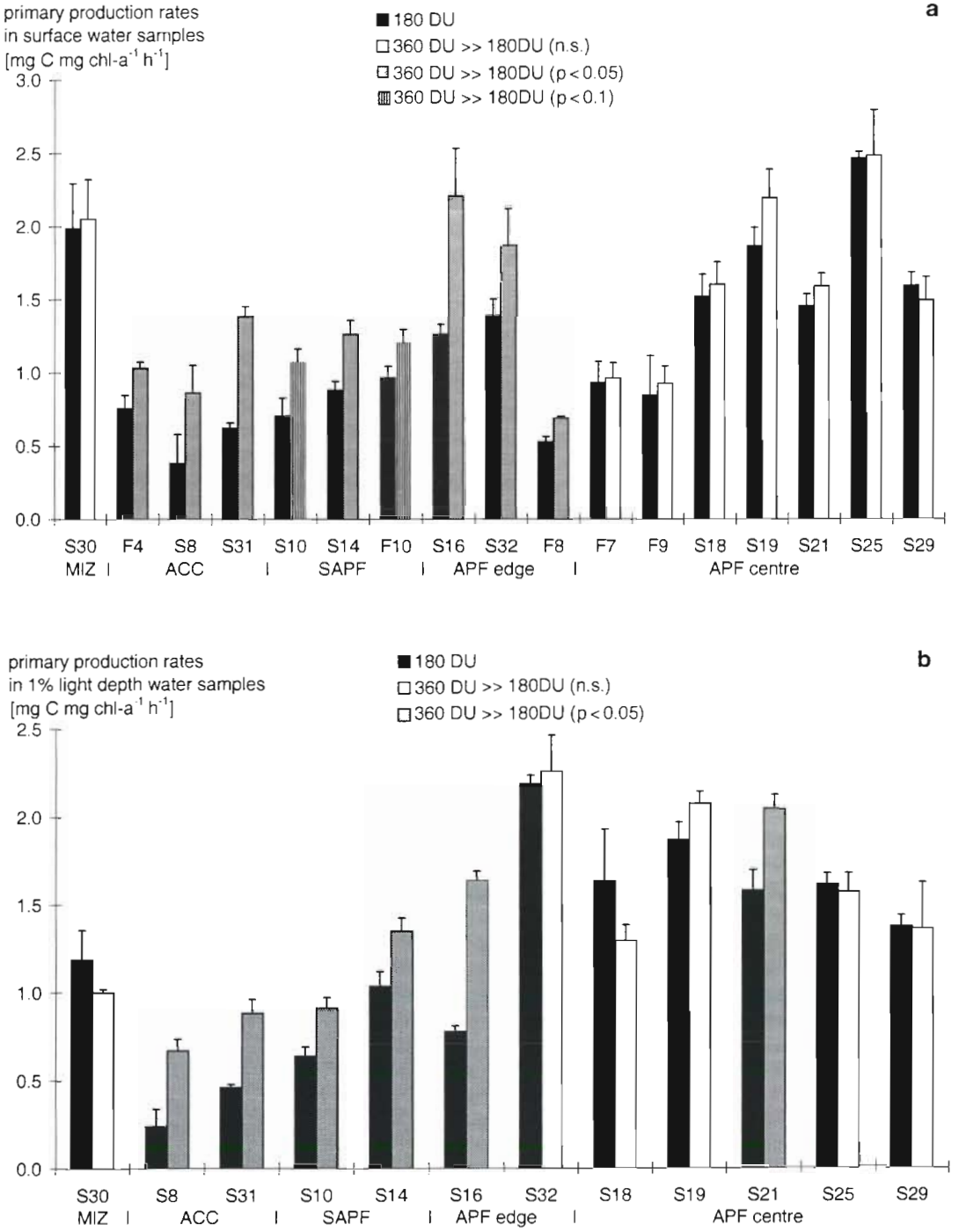

Fig. 6. Primary production rates after 4 h incubation under a spectrum corresponding to an irradiance field encountered at 5 m depth under depleted (180 DU) and normal ozone concentrations (360 DU) (a) in surface water samples and (b) in 1 % light depth water samples. Grey bars: stations showing a significantly higher ($p < 0.05$) production rate under normal ozone concentration conditions as compared to depleted ozone concentration conditions (360 DU >> 180 DU); striped bars: $p < 0.1$; open bars: no significant difference between the two. Stations are grouped to the areas within the Atlantic sector of the Southern Ocean in which they are located: MIZ, ACC, SAPF, APF edge (within the APF, with high biomass but already low surface temperatures), APF centre

B radiation due to high levels of ozone concentrations (>360 DU). Transitions into and out of the 'ozone hole' occur at time scales of several days (Roy et al. 1994). During our cruise the actual ozone concentrations were in between the extremes we used for our incubations.

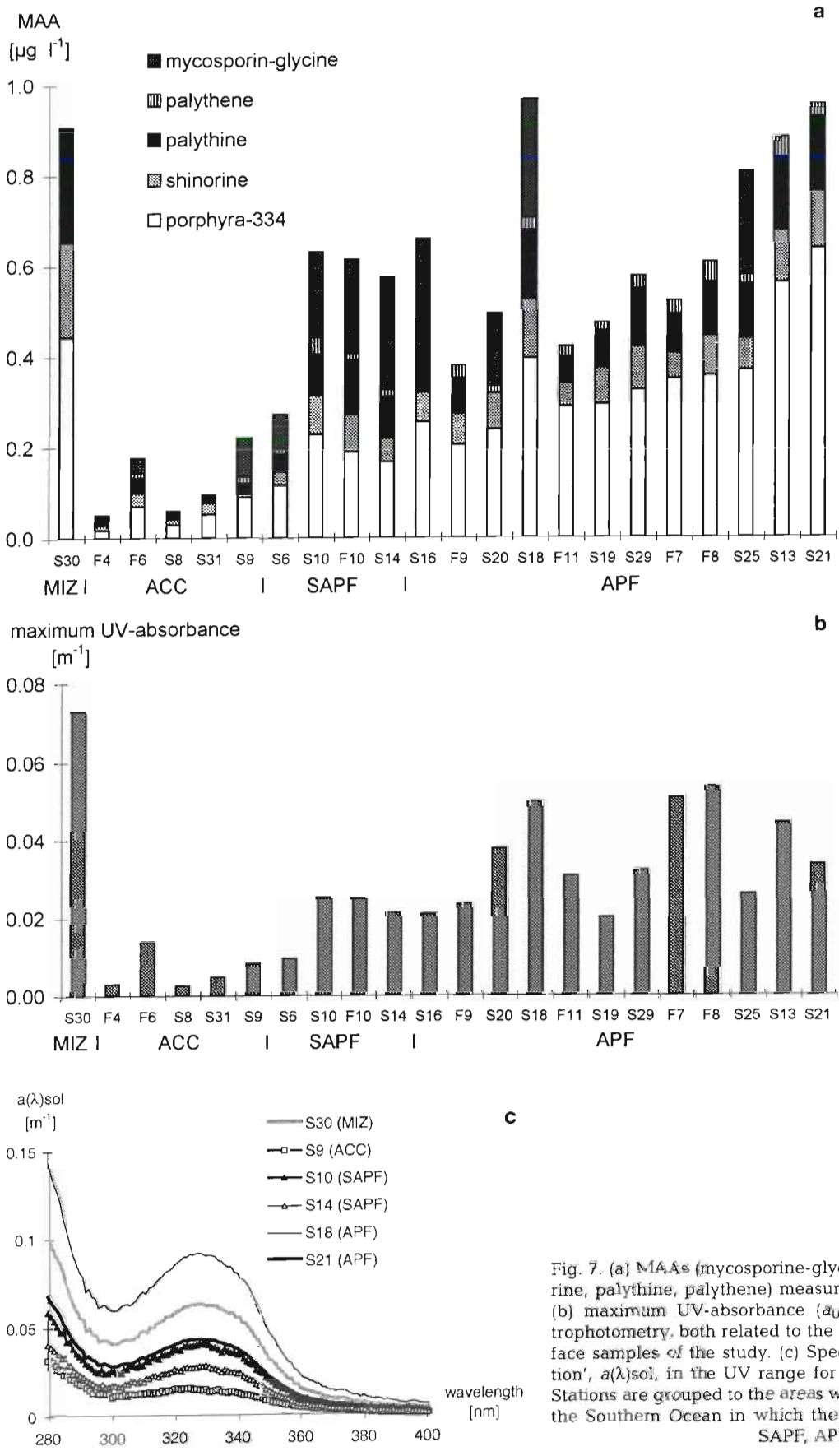

Fig. 7. (a) MAAs (mycosporine-glycine, porphyra-334, shinorine, palythine, palythene) measured by HPLC analysis and (b) maximum UV-absorbance (a_{UV}sol) measured by spectrophotometry, both related to the filtered volume, in all surface samples of the study. (c) Spectra of 'unpacked absorption', $a(\lambda)$sol, in the UV range for 6 representative stations. Stations are grouped to the areas within the Atlantic sector of the Southern Ocean in which they are located: MIZ, ACC, SAPF, APF

Impact of increased UVR

Studying the effects of naturally enhanced UVR due to stratospheric ozone depletion on both photosynthetic parameters, the relative quantum yield of electron transport in PSII, F_v/F_m, and primary production rates, helps to elucidate inhibitory and damaging processes on photosynthesis. Nilawati et al. (1997) also studied these 2 parameters in phytoplankton from Alaska, but used fluence rates of UV-B which accounted only for 10% of typical midday, surface-incident radiation measured during May. Under conditions corresponding to depleted stratospheric ozone concentrations, F_v/F_m decreased significantly for all samples from our study as compared to its value under conditions simulating normal ozone concentrations. Kroon et al. (1994) also measured the UV-B-specific decrease in quantum yield in springtime ice algae from the Southern Ocean. Similar results have been obtained in pennate diatoms by Nilawati et al. (1997) and in macroalgae by Hanelt et al. (1997) and Bischof et al. (1998).

Neale et al. (1993) pointed out that PSII electron transport is very susceptible to UV-B inhibition. Depending on recovery time, lower F_v/F_m rates may either be a result of photoinhibition or photodamage (Osmond 1994); photoinhibition is defined as a protective mechanism which causes an active down-regulation of photosynthesis as opposed to passively induced photodamage. Measurements of the kinetics of recovery can reveal whether UV exposure causes fast reversible down-regulation of photosynthetic activity similar to the inhibition of PAR. Dynamic photoinhibition amplifies the non-photochemical energy dissipation so that excessively absorbed energy, which is not utilised in photochemistry, is converted into harmless thermal radiation (Krause & Weis 1991, Hanelt 1996). Chronic photoinhibition is related to the rate of damage of the D_1 protein, which exceeds its rate of repair, resulting in a breakdown (degradation) of the D_1 protein and a loss of photosynthetic activity (Mattoo et al. 1984, Ohad et al. 1984, Krause 1988, Andersson et al. 1992). Fast recovery during the afternoon is indicative of photoprotection, whereas photodamage of proteins and pigments would require several days of repair (Hanelt et al. 1992).

For all samples studied here F_v/F_m remained low after keeping the incubated samples in the dark (over 4 h). The control ($t0$) and the low UV light-incubated samples had similar F_v/F_m values. Greenberg et al. (1989) found that the repair system of PSII only works under either PAR or UV-A + PAR irradiance. Therefore, after high UV-light incubation F_v/F_m of the phytoplankton samples did not increase in the dark. Within the blooms, the decrease in F_v/F_m was probably caused by dynamic photoinhibition due to enhanced UVR; in contrast, in the areas outside the blooms, the production rates also decreased significantly. Here, besides a breakdown (degradation) of the D_1 protein, RUBISCO was also probably down-regulated, resulting in at least chronic photoinhibition. If recovery did not occur within hours, UVR probably caused photodamage. Lesser et al. (1996) found that the 20% decrease in the RUBISCO pool in the cultures held in UV-transmitting enclosures was comparable to the 22% decrease in light-saturated rates of photosynthesis. They showed that solar UVR can induce decreases in RUBISCO, a phenomenon which had been only reported before for plants exposed to artificial UVR sources. It is still unknown if RUBISCO is a direct target of UV damage or if it is down-regulated as a result of chronic damage to other components. Except for 2 stations (S21, S32), surface samples and the sample at the 1% light depth showed the same reaction to enhanced UVR. Therefore it can be concluded that surface samples were not inhibited prior to the incubation.

It should be pointed out that interactive effects of UVR and iron limitation on phytoplankton photosynthesis have been found (Takeda & Kamatani 1989, Auclair 1995). However, iron concentrations were low (<1 nM) at all sites during our cruise (de Jong et al. 1997) and were therefore unlikely to influence the differences in reactions to enhanced UVR.

Role of UV absorbing compounds

We observed the highest concentrations of MAAs and a_{UV}sol values at a few sites within the APF and the MIZ and lowest concentrations in the ACC. The concentration of UV-absorbing compounds does not alone determe the efficiency to screen UV radiation from vulnerable targets within the cell; the organismal size is also a major determinant (Karentz et al. 1991, Garcia-Pichel 1994, Riegger & Robinson 1997). Size fractionated data of chl *a* (Bracher et al. 1999) show that the algal class >20 µm was dominant, with over 60% at both bloom sites. At the SAPF and within the ACC, the <20 and >2 µm fractions increased up to 70% and the >20 µm fractions decreased to 10%. Garcia-Pichel (1994) calculated in his bio-optical model that the smallest phytoplankters are the most sensitive to UV-B. The model predicts that sunscreens cannot be used as a photoprotective mechanism of any relevance by picoplankters (cell diameter <2 µm). Conversely, the microplankters (cell diameter 20 to >200 µm) can use sunscreens with efficiencies comparable to well-studied damage-repair mechanisms. Among nanoplankters (cell diameter 2 to 20 µm), sunscreens can afford considerable benefits but only at the expense of relatively

heavy investments and with restricted efficiencies. Riegger & Robinson (1997) found an increased potential for sunscreen protection with cell size among Antarctic diatoms in their study on photoinduction of UV-absorbing compounds. Garcia-Pichel (1994) claims that for any cell with a diameter of <20 µm efficient protection against enhanced UVR is only achieved with investment >10% of the dry biomass. Karentz et al. (1991) and Karsten et al. (1998) found in extensive surveys of marine organisms from field populations, mostly metazoans and macroalgae, specific contents of UV-absorbing MAAs to be <1% of the dry weight in all cases. Investments of 10% of dry biomass to respond to a single ecological factor (e.g., close to the investment in total cellular nucleic acids) would be highly inefficient and should be considered physiologically implausible under conditions of balanced growth.

Therefore, in our study, probably only within the phytoplankton blooms, where large cells (at the APF) or big colonies (at the MIZ) were dominating, were MAAs acting as efficient protectors against enhanced levels of UVR. Besides the lower sunscreen effect of MAAs in small cells, these phytoplankters are more vulnerable to UV exposure compared to large cells. The larger the cell, the longer the optical path through the cell and the more likely light will be absorbed before 'hitting' too many subcellular targets. In addition, due to a much higher cell density in phytoplankton blooms compared to conditions outside of blooms, selfshading is high. Therefore, relatively less irradiance, including UV-B, reaches the particular cells.

Vertical mixing

Helbling et al. (1994) found that the physical characteristics of the upper water column play an important role in explaining the variability in Antarctic primary production attributable to UVR. Cullen & Lesser (1991) have demonstrated that for equal doses of UV-B, short exposures to high irradiance are more damaging than longer exposure to lower irradiance. Consequently, in a rapidly mixing water column, UVR damage to phytoplankton that are approaching the surface may be particularly acute, especially in light of the lag time observed for the induction of MAA accumulation (Riegger & Robinson 1997). Alternatively, the ratios of UV-A/UV-B and blue light/UV-B increase with depth (Smith et al. 1992). Riegger & Robinson (1997) have shown that the production of MAAs in Antarctic diatoms and *Phaeocystis antarctica* is a light-controlled process that displays a wavelength-dependent response, but peak responses are at wavelengths somewhat longer (345 to 460 nm) than those inflicting the greatest damage (<330 nm). Therefore, for ascending phytoplankton exhibiting a MAA induction response in the UVA/blue portion of the spectrum, their data indicate that the accumulation of MAAs begins at depth before the cells rise near the surface, where the UV-B damage is greater. As said above, the repair system of PSII only works under either PAR or UV-A + PAR irradiance (Greenberg et al. 1989). Mixing to depths below where UV-B reaches a significant amount (<20 m Prezelin et al. 1994), but still within the euphotic zone (in our study between 30 and 70 m), may implicate that turnover rates of recovery in phytoplankton photosynthesis can be high enough to compensate for the UV damage.

In our study upper mixed layers (UMLs) were shallow within the phytoplankton blooms (within the MIZ 10 to 15 m and within the APF 15 to 35 m), while in the SAPF they always extended to depths exceeding 35 m and in the ACC outside of frontal systems 50 m (Strass et al. 1997). In a stable and shallow UML phytoplankton apparently has the capability and time required to acclimate to other light conditions (e.g., by induction of MAA synthesis and repair cycles) and to become fairly resistant to UVR. This might be another explanation why in our study only production rates outside the blooms decreased significantly. Helbling et al. (1994) found, in their broad study looking at UV effects on Antarctic phytoplankton, photosynthesis to be markedly inhibited due to UVR when samples were collected from a water column where the density increased continuously with depth: about 80% enhancement when UV-B was cut off and 350% when both UV-B and UV-A were removed. However, when a distinct and relatively shallow pycnocline was present, almost no inhibition was noticed when the samples came from the UML, but samples from below the UML showed inhibition due to UVR.

Acknowledgements. The authors would like to thank C. Bratrich, R. Lehmann, the crew and captain of RV 'Polarstern' and chief scientist V. Smetacek for their support during ANTXIII/2. Special thanks for help and instructions to T. Sawall and U. Karsten with the MAA analysis, to D. Hanelt and B. Kroon with the PAM fluorometer and to H. Tüg, T. Hanken, N. Rieper and R. Roettgers with the solar simulator. We thank I. Ewen, I. Hense and M. Lucas for chlorophyll analysis and I. Zondervan for DIC analysis. M. Tilzer and H. Tüg provided critical comments on the manuscript. This research was supported by the Alfred Wegener-Institute for Polar and Marine Research. This is AWI contribution number 1676.

LITERATURE CITED

Abele-Oeschger D, Tüg H, Röttgers R (1997) Dynamics of UV-driven hydrogen peroxide formation on an intertidal sandflat. Limnol Oceanogr 42:1406–1415

Andersson B, Salter AH, Virgin I, Vass I, Styring S (1992) Photodamage of photosystem II–primary and secondary events. J Photochem Photobiol B Biol 15:15–21

Auclair JC (1995) Implications of increased UV-B induced photoreduction: Iron (II) enrichment stimulates picocyanobacterial growth and the microbial food web in clear-water acidic Canadian Shield lakes. Can J Fish Aquat Sci 52:1782–1788

Bischof K, Hanelt D, Wiencke C (1998) UV radiation can affect depth-zonation of Antarctic macroalgae. Mar Biol 131:597–605

Boucher NP, Prezelin BB (1996) An *in situ* biological weighing function for UV inihibition of phytoplankton carbon fixation in the Southern Ocean. Mar Ecol Prog Ser 144: 223–236

Bracher AU, Tilzer MM (2000) Underwater light field and phytoplankton absorbance in different zones of the Southern Ocean during early summer 1995/1996. Deep-Sea Res II: (in press)

Bracher AU, Kroon BMA, Lucas MI (1999) Primary production, physiological state and composition of phytoplankton in the Atlantic sector of the Southern Ocean. Mar Ecol Prog Ser 190:1–16

Carreto JI, Carignan MO, Daleo G, de Marco SG (1990) Occurrence of mycosporine-like amino acids in the red-tide dinoflagellate *Alexandrium excavatum*: UV-photoprotective compounds? J Plankton Res 12:909–921

Cullen JJ, Lesser MP (1991) Inhibition of photosynthesis by ultraviolet radiation as a function of dose and dosage rate: results from a marine diatom. Mar Biol 111:183–190

Davidson AT, Marchant HJ (1994) The impact of ultraviolet radiation on *Phaeocystis* and selected species of Antarctic marine diatoms. Antarct Res Ser 62:187–205

Davidson AT, Marchant HJ, de la Mare WK (1996) Natural UVB exposure changes the species composition of Antarctic phytoplankton in mixed culture. Aquat Microb Ecol 10: 299–305

de Jong JTM, den Das J, Timmermans KR, de Baar HJW (1997) Field distribution of iron in a section of the Antarctic Polar Frontal Zone. Rep Polar Res 221:53–61

Dunlap WC, Chalker BE (1986) Identificaton and quantification of near-UV absorbing compounds (S-320) in a hermatypic scleractinian. Coral Reefs 5:155–159

Dunlap WC, Chalker BE, Oliver JK (1986) Bathymetric adaptations of reef-building corals at Davies Reef, Great Barrier Reef, Australia, III, UV-B absorbing compounds. J Exp Mar Biol Ecol 104:239–248

Ekelund NG (1994) Influence of UV-B radiation on photosynthetic light-response curves, absorption spectra and motility of four phytoplankton species. Physiol Plant 91: 696–702

El-Sayed SZ, Stephens FC, Bidigare RR, Ondrusek ME (1990) Effects of ultraviolet radiation on Antarctic marine phytoplankton. In: Kerry KR, Hempel G (eds) Antarctic ecosystems. Ecological change and conservation. Springer-Verlag, Heidelberg, p 379–385

Evans CA, O'Reilly JE, Thomas JP (1987) A handbook for the measurement of chlorophyll *a* and primary production. In: Biological investigations of marine antarctic systems and stocks (biomass), Vol 8. Texas A&M University, College Station, TX, p 47–107

Frederick JE, Snell HE (1988) Ultraviolet radiation levels during Antarctic spring. Science 241:438–440

Garcia-Pichel F (1994) A model for internal self-shading in planktonic organisms and its implications for the usefulness of ultraviolet sunscreens. Limnol Oceanogr 39:1704–1717

Garcia-Pichel F, Castenholz RW (1993) Occurrence of UV-absorbing, mycosporine-like compounds among cyanobacterial isolates and an estimate of their screening capacity. Appl Environ Microbiol 59:163–169

Gleason DF (1993) Differential effects of ultraviolet radiation on green and brown morphs on the Caribbean coral *Porites astreoides*. Limnol Oceanogr 38:1452–1463

Greenberg BM, Gaba V, Canaani O, Malkin S, Mattoo AK, Edelman M (1989) Separate photosynthesizers mediate degradation of the 32-kDa photosystem II reaction center protein in the visible and UV spectral regions. Proc Natl Acad Sci USA 86:6617–6620

Hanelt D (1996) Photoinhibition of photosynthesis in marine macroalgae. Sci Mar 60:243–248

Hanelt D, Huppertz K, Nultsch W (1992) Photoinhibition of photosynthesis and its recovery in red algae. Bot Acta 105: 278–284

Hanelt D, Wiencke C, Nultsch W (1997) Influence of UV radiation on the photosynthesis of Arctic macroalgae in the field. J Photochem Photobiol B 38:40–47

Helbling EW, Villafañe V, Ferrario M, Holm-Hansen O (1992) Impact of natural ultraviolet radiation on rates of photosynthesis and on specific marine phytoplankton species. Mar Ecol Prog Ser 80:89–100

Helbling EW, Villafañe V, Holm-Hansen O (1994) Effects of ultraviolet radiation on antarctic marine phytoplankton photosynthesis with particular attention to the influence of mixing. In: Weiler CS, Penhale PA (eds) Ultraviolet radiation in Antarctica: measurements and biological effects. Antarct Res Ser 62:207–227

Helbling EW, Chalker BE, Dunlap WC, Holm-Hansen O, Villafañe VE (1996) Photoacclimation of Antarctic marine diatoms to solar ultraviolet radiation. J Exp Mar Biol Ecol 204:85–101

Hense I, Bathmann U, Hartmann C (1998) Spiny phytoplankton—slowing down the carbon pump in the Southern Ocean? EOS (Trans Am Geophys Union) 79:89

Holm-Hansen O, Helbling E, Lubin D (1993) Ultraviolet radiation in Antarctica: inhibition of primary production. Photochem Photobiol 58:567–570

Ito S, Hirata Y (1977) Isolation and structure of mycosporine from zoanthid *Palythoa tuberculosa*. Tetrahedron Lett 28: 2429–2430

Iwanzik W, Tevini M, Dohnt G, Voss M, Weiss W, Graber P, Renger G (1983) Action of UV-B radiation on photosynthetic primary reactions in spinach chloroplasts. Physiol Plant 58:401–407

JGOFS (1993) Measurements of algal chlorophylls and carotenoids by HPLC. In: Measurement protocols JGOFS. SCOR-UNESCO Publ, Paris, p 72–79

Karentz D, Mc Euen FS, Land MC, Dunlap WC (1991) Survey of mycosporine-like amino acid compounds in Antarctic marine organisms: potential protection from ultraviolet exposure. Mar Biol 108:157–166

Karsten U, Sawall T, Hanelt D, Bischof K, Figueroa FL, Flores-Moya A, Wiencke C (1998) An inventory of UV-absorbing mycosporine-like amino acids in macroalgae from polar to warm-temperate regions. Bot Mar 41:443–453

Krause GH (1988) Photoinhibition of photosynthesis. An evaluation of damaging and protective mechanisms. Physiol Plant 74:566–574

Krause GH, Weis E (1991) Chlorophyll fluorescence and photosynthesis: the basics. Annu Rev Plant Physiol Plant Mol Biol 42:313–349

Kroon B, Schofield O, Prezelin BB (1994) UV-B specific decreases in photosystem II quantum yield in a field community of Antarctic ice algae under natural daylight. EOS 75:85

Labs D, Neckel H (1984) The solar radiation between 3300 and 18500 Angström. Solar Phys 90:205–258

Labs D, Neckel H, Simon PC, Thuillier G (1987) Ultraviolet solar irradiance measurements from 200 to 358 nm during Spacelab 1 mission. Solar Phys 107:203–219

Lesser MP, Cullen JJ, Neale PJ (1994) Carbon uptake in a marine diatom during acute exposure to ultraviolet B radiation: relative importance of damage and repair. J Phycol 30:183–192

Lesser MP, Neale PJ, Cullen JJ (1996) Acclimation of Antarctic phytoplankton to ultraviolet radiation: ultraviolet-compounds and carbon fixation. Mol Mar Biol Biotechnol 5: 314–325

Lucas MI, Bury S, Tremblay JE, Bracher A, Lehmann R, Bratrich C, Ewen I (1997) Primary production, nitrogen cycling and photosynthesis-irradiance relationships for phytoplankton associated with the Antarctic polar front in summer. Rep Polar Res 221:78–101

Mattoo AK, Hoffman-Falk H, Marder JB, Edelman M (1984) Regulation of protein metabolism: coupling of photosynthetic electron transport *in vivo* degradation of therapidly metabolised 32-kilodalton protein of the chlorophyll membranes. Proc Natl Acad Sci USA 81:1380–1384

Nakamura H, Kobayashi J, Hirata Y (1982) Separation of micosporine-like amino acids in marine organisms using reversed-phase high-performance liquid chromatography. J Chromatogr 250:113–118

Neale PJ, Lesser MP, Cullen JJ (1992) Detecting UV-induced inhibition of photosynthesis in Antarctic phytoplankton. Antarct J US 27:122–124

Neale PJ, Cullen JJ, Lesser MP, Melis A (1993) Physiological bases for detecting and predicting photoinhibition of aquatic photosynthesis by PAR and UV radiation. In: Yamamoto HY, Smith CM (eds) Photosynthetic responses to the environment. Am Soc Plant Physiol, Rockville, MD, p 61–77

Neale PJ, Lesser MP, Cullen JJ (1994) Effects of ultraviolet radiation on the photosynthesis of phytoplankton in the vicinity of McMurdo Station, Antarctica. Antarct Res Ser 62:125–142

Nilawati J, Greenberg BM, Smith REH (1997) Influence of ultraviolet radiation on growth and photosynthesis of two cold ocean diatoms. J Phycol 33:215–224

Nogues S, Baker NR (1995) Evaluation of the role of damage to photosystem II in the inhibition of CO_2 assimilation in pea leaves on exposure to UVB radiation. Plant Cell Environ 18:781–787

Ohad I, Kyle DJ, Arntzen CJ (1984) Membrane protein damage and repair: removal and replacement of inactivated 32-kilodalton polypeptides in chloroplast membranes. J Cell Biol 99:481–485

Osmond CB (1994) What is photoinhibition? Some insights from comparisons of shade and sun plants. In: Baker NR, Bowyer NR (eds) Photoinhibition of photosynthesis, from the molecular mechanisms to the field. Oxford University Press, Oxford, p 1–24

Prezelin BB, Boucher NP, Smith RC (1994) Marine primary production under the influence of the Antarctic ozone hole: Icecolors '90. In: Weiler CS, Penhale PA (eds) Ultraviolet radiation in Antarctica: measurements and biological effects. Antarct Res Ser 62:159–186

Riegger L, Robinson D (1997) Photoinduction of UV-absorbing compounds in Antarctic diatoms and *Phaeocystis antarctica*. Mar Ecol Prog Ser 160:13–25

Rieper N (1996) Steuerung eines Sonnenscheinsimulators über das Extinktionsverhalten eines 3-stufigen Flüssigkeitsfilter. Simulationsprogramm und Steuerelektronik. Diploma Thesis, Cuxhaven

Roy CR, Gies HP, Tomlinson DW, Lugg DL (1994) Effects of ozone depletion on the ultraviolet radiation environment at the Australian stations in Antarctica. In: Weiler CS, Penhale PA (eds) Ultraviolet radiation in Antarctica: measurements and biological effects. Antarct Res Ser 62:1–15

Ryan KG (1992) UV radiation and photosynthetic production. J Photochem Photobiol 13:235–240

Schofield O, Kroon BMA, Prezelin BB (1995) Impact of ultraviolet radiation on photosystem II activity and its relationship to the inhibition of carbon fixation rates for Antarctic ice algae communities. J Phycol 31:703–715

Schreiber U, Hormann H, Neubauer C, Klughammer C (1995) Assessment of photosystem II photochemical quantum yield by chlorophyll fluorescence quenching analysis. Aust J Plant Physiol 22:209–220

Shick JM, Dunlap WC, Chalker BE, Banaszak AT, Rosenzweig TK (1992) Survey of ultraviolet radiation-absorbing mycosporine-like amino acids in organs of coral reef holothuroids. Mar Ecol Prog Ser 90:139–148

Smith RC, Baker KS (1978) Optical classification of natural waters. Limnol Oceanogr 23:260–267

Smith RC, Baker KS (1981) Optical properties of the clearest natural waters (200–800 nm). Appl Optics 20:177–184

Smith RC, Prezelin BB, Baker KS, Bidigare RR, Boucher NP, Coley T, Karentz D, MacIntyre S, Matlick HA, Menzies D, Ondrusek M, Wan Z, Waters KJ (1992) Ozone depletion: ultraviolet radiation and phytoplankton biology in Antarctic waters. Science 255:952–959

Sosik HM, Mitchell BG (1991) Absorption, fluorescence, and quantum yield for growth in nitrogen-limited *Dunaniella tertiolecta*. Limnol Oceanogr 36:910–921

Stochaj WR, Dunlap WC, Shick JM (1994) Two new UV-absorbing mycosporine-like amino acids from the sea anemone *Anthopleura elegantissima* and the effects of zooxanthellae and spectral irradiance on chemical composition and content. Mar Biol 118:149–156

Stoll M, Zondervan I, de Jong E (1997) The carbon dioxide system in Antarctic waters. Rep Polar Res 221:64–67

Strass V, Timmermann R, Fischer H, Hofmann M, Gwilliam P, Wischmeyer A (1997) CTD stations and water bottle sampling. Rep Polar Res 221:34–39

Strickland JDH, Parsons TR (1972) A practical handbook of seawater analysis. Bull Fish Res Board Can 167

Strid A, Chow WS, Anderson JM (1990) Effects of supplementary ultraviolet-B radiation on photosynthesis in *Pisum sativum*. Biochim Biophys Acta 1020:260–268

Takano S, Uemura D, Hirata Y (1978a) Isolation and structure of a new amino acid, palythine, from the zoanthid *Palythoa tuberculosa*. Tetrahedron Lett 26:2299–2300

Takano S, Uemura D, Hirata Y (1978b) Isolation and structure of two new amino acids, palythinol and palythene, from the zoanthid *Palythoa tuberculosa*. Tetrahedron Lett 49:4909–4912

Takano S, Nakanishi A, Uemura D, Hirata Y (1979) Isolation and structure of a UV-absorbing substance, porphyra-334 from the red alga *Porphyra tenera* Kjellmann. Chem Lett 25:419–420

Takeda S, Kamatani A (1989) Photoreduction of Fe(III)-EDTA complex and its availability to the coastal diatom *Thalassiosira weissflogii*. In: Okaichi T, Anderson DM, Nemoto T (eds) Red tides: biology, environmental science and toxicology. 1. International Symposium on Red Tides, Takamatsu, p 349–352

Tevini M (1994) Physiological changes in plants related to UV-B radiation: an overview. In: Biggs RH, Joyner MEB (eds) Stratospheric ozone depletion/UV-B radiation in the biosphere. Springer-Verlag, Berlin, p 37–56

Tsujino I, Yabe K, Sekekawa I (1980) Isolation and structure of a new amino acid, shinorine, from the red algae *Chondrus yendoi* Yamada et Mikami. Botanica Mar 23:65–68

Tüg H (1978) Absolut- und Relativanschluß südlicher Standardsterne: Berechnung des solaren Strahlungstransfers. PhD thesis, Bochum

Tüg H (1996) Solar simulation. Ann Rep AWI Pol Mar Res 1994/1995:43–46

Vincent WF, Roy S (1993) Solar ultraviolet-B radiation and aquatic primary production: damage, protection, and recovery. Environ Rev 1:1–11

Wilson MI, Gosh S, Gerhardt KE, Holland N, Sudhakar Babu T, Ededlman M, Dumbroff EB, Greenberg BM (1995) *In vivo* photomodification of ribulose-1,5-biphosphate carboxylase/oxygenase holoenzyme by ultraviolet-B radiation. Plant Physiol 109:221–229

Editorial responsibility: Osmund Holm-Hansen, (Contributing Editor), La Jolla, California, USA

Submitted: June 15, 1998; Accepted: September 20, 1999
Proofs received from author(s): March 27, 2000